DOI: 10.1002/adma.200702981

Plasma-Polymerized Multistacked Organic Bipolar Films: A New Approach to Flexible High-κ Dielectrics**

By *Dhiman Bhattacharyya, Woo-Jun Yoon, Paul R. Berger,** and *Richard B. Timmons**

Organic-based flexible dielectric films with high permittivity (ε) are desirable for future applications of organic thin-film transistors, such as smartcards and radio frequency identification (RFID) tags, that concurrently desire flexible or conformable substrates. Advances in the development of all-polymer field-effect transistors (PFETs) have been particularly significant for their potential in a flexible form. Major improvements have been reported for both the semiconductor and the dielectric components of PFETs.[1] For example, with respect to semiconductor considerations, noteworthy gains have been achieved in increasing carrier mobility and in identifying lower-cost production technology, however, PFET operational voltages tend to be too high for the intended portable applications. But the voltages could be significantly lowered if a suitable dielectric with a high dielectric constant (k), compatible with the PFET process and in a flexible form factor with thicknesses that is controllably thin, was identified.

This Communication focuses on the organic dielectric film component of PFETs, required for all-polymer PFETs by tailoring high-k polymer films. The much-needed advances in this area pose difficult challenges in terms of materials science considerations. One such problem centers on the fact that organic films are inherently low-k; having k values significantly less than those of ceramic (inorganic) materials. Additionally, leakage currents through the film also pose potential problems given the generally porous nature of organic based polymeric films. On the other hand, organic films offer far more favorable prospects to satisfy flexibility requirements envisioned for many inexpensive all-polymeric devices.

As in the case of the semiconductor research, development of organic-based dielectrics has received increasing attention in recent years.[2–6] A number of innovative approaches have been explored, and encouraging results have been obtained. An example of a recent notable advance in this area is the development of σ–π molecular organosiloxane dielectric multilayers having very low threshold voltages and high k values ($k \approx 16$).[7] Another frequently employed approach is to increase the k values of organic films by incorporation of ceramic fillers.[8,9] Although these fillers can provide a substantial increase in k, they simultaneously introduce undesirable complications associated with interactions in the composite inorganic–organic film, leading to increased porosity and, ultimately, poor adhesion between the composite and the purely organic circuit boards. More recently, an interesting report has described polymer composite films containing silver metal (Ag) nanoparticles, with the metal loading approaching the percolation threshold.[10] The Ag particles were coated with a carbonaceous layer to prevent interparticle electrical contact and to improve compatibility between the polymeric matrix and the filler particles. Very favorable electrical properties, (k values, breakdown voltages, leakage current) were measured for these composite dielectric films. However, it is not clear at this time if these composite materials will exhibit long-term stability, in that particle aggregation over time would be a concern because the particles are not covalently bound to the polymer matrix molecules.

The present study involves an innovative approach to synthesis of totally organic dielectric films based on multilayered bipolar films produced by plasma-enhanced chemical vapor deposition (PECVD). The layered structures were obtained by successive polymerization of a carboxylic acid monomer followed by that of an amine containing monomer. The process involves production of alternating ultrathin layers of each monomer to create the bipolar interfaces between layers as achieved by spontaneous proton transfer from the acid to the amine. Scheme 1 provides a simple visualization of the nature of the bipolar interface between the two films. A radio frequency (RF) pulsed plasma reactor system was employed to provide deposition conditions that permit retention of the requisite monomer functionalities (i.e., –COOH and $-NH_2$ groups) while simultaneously providing improved film thickness control over that encountered under

[*] Prof. P. R. Berger, W.-J. Yoon
Department of Electrical and Computer Engineering
The Ohio State University
Columbus, OH 43210 (USA)
E-mail: pberger@ieee.org

Prof. P. R. Berger
Department of Physics
The Ohio State University
Columbus, OH 43210 (USA)

Prof. R. B. Timmons, D. Bhattacharyya
Department of Chemistry and Biochemistry
University of Texas at Arlington
700 Planetarium Place, Arlington, TX 76019 (USA)
E-mail: timmons@uta.edu

[**] D.B. and W.-J.Y. contributed equally to this work. This work was partially supported by the NSF (DMR-0103248) and by the Center for Photovoltaics Innovation and Commercialization (OSU), and by the AFOSR and AFRL (UTA).

© 2008 WILEY-VCH Verlag GmbH & Co. KGaA, Weinheim

WILEY InterScience DISCOVER SOMETHING GREAT

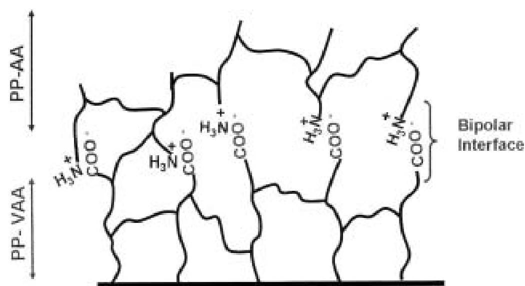

Scheme 1. Schematic diagram of the interfacial boundary between the plasma-polymerized allyl amine (PP-AA) and vinylacetic acid (PP-VAA) thin films.

conventional continuous wave (CW) plasma operations.[11–13] Film characterization, using X-ray photoelectron spectroscopy (XPS) and attenuated total reflectance Fourier transform IR (ATR FT-IR) spectroscopy, provide unequivocal evidence for the presence of the $–COO^-$ and $–NH_3^+$ polar entities as shown in Figures 1 and 2, respectively.

Figure 1 shows a compilation of high-resolution XPS data for C1s (panels 1A–1C), N1s (panels 2A, 2B), and O1s (panels 3A, 3B). Spectra of polymer films obtained from pure allyl amine and vinylacetic acid, along with the assigned chemical functionalities, are shown in panels 1A and 1B. These spectra can be contrasted with the C1s spectrum recorded when a thin polyallyl amine film (2 nm) was deposited onto a polyvinylacetic acid film (panel 1C). As shown in 1C, the high binding energy –COOH peak (at 289 eV) has been broadened and the peak maximum shifted to a slightly lower binding energy of 288.5 eV, a shift that is consistent with the formation of COO^- groups. The high-resolution N and O atom spectra provide additional verification of the formation of polar groups. The N1s spectra reveal the presence of a peak at 401.7 eV in the layered film (panel 2B) not present in the pure allyl amine film (panel 2A). This high-binding-energy peak is consistent with the presence of ammonium ion functionality. Finally, the high-resolution O1s spectrum of the layered film reveals a low-binding-energy peak at 531.7 eV, which is not present in the film obtained from pure vinylacetic acid. This low-

Figure 1. 1A–1C) High-resolution C1s X-ray photoelectron spectra of plasma-polymerized allyl amine (PP-AA), vinylacetic acid (PP-VAA), and the double-layer bipolar film, respectively. 2A,2B) High-resolution N1s spectra for PP-AA and the double layer bipolar film, respectively. 3A,3B) High-resolution O1s spectra for PP-VAA and the double layer bipolar film; respectively.

© 2008 WILEY-VCH Verlag GmbH & Co. KGaA, Weinheim

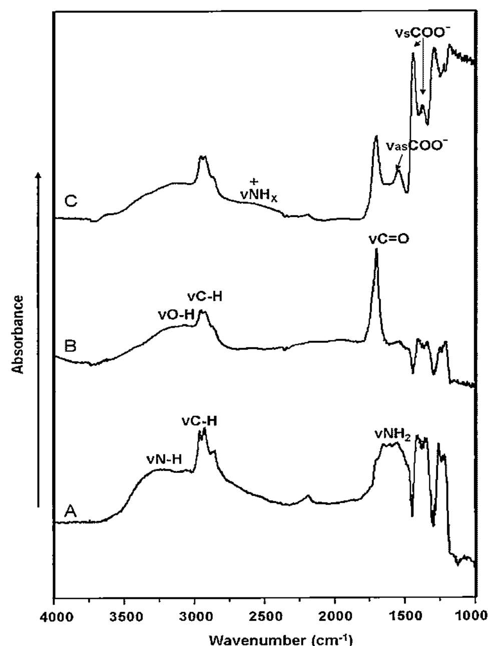

Figure 2. ATR-FTIR spectra of plasma-polymerized A) allyl amine (PP-AA), B) vinylacetic acid (PP-VAA), and C) the double layer bipolar film.

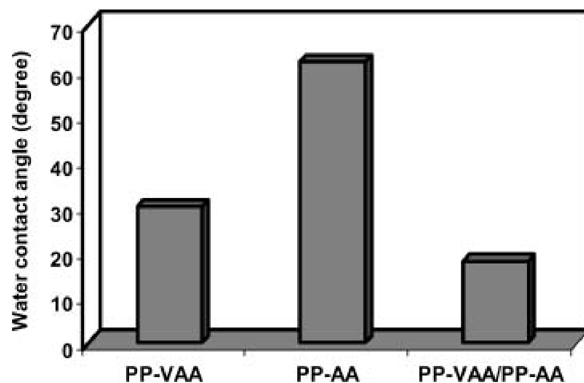

Figure 3. Static sessile-drop water contact angle measurements with plasma polymerized allyl amine (PP-AA), vinylacetic acid (PP-VAA) and the double layer bipolar film (PP-VAA/PP-AA).

binding-energy peak is also consistent with the presence of COO^- groups in the layered film.

ATR FT-IR absorption spectral studies provide additional confirmation of the presence of a bipolar film. In these experiments, an ultrathin (2 nm) polyallyl amine film was again deposited onto an equally thin 2 nm polyvinylacetic acid film, using a silicon substrate.[14] A comparison of the ATR-FT-IR spectrum of this composite sample with spectra of pure polyallyl amine and polyvinylacetic acid is shown in Figure 2. Of special significance are the appearance of characteristic $-COO^-$ and NH_x^+ absorption bands, as indicated in Figure 2c, which are not present in the pure polyallyl amine (Fig. 2b) or the pure polyvinylacetic acid films (Fig. 2b).

Additionally, static sessile water drop contact-angle measurements revealed the composite film to be significantly more wettable than either pure polyallyl amine and polyvinylacetic acid single-layer films, as shown in Figure 3. The increased wettability of the composite film would be in accord with expectations based on the polar nature of these films in light of the presence of the positive and negative ion centers.

A variety of samples containing alternating thin layers of the –COOH and $-NH_2$ polymers were deposited on a p-doped Si substrate for use in determination of the dielectric and electrical properties of these bipolar containing films. Three different sets of samples containing alternating layers of the –COOH and $-NH_2$ films were prepared. The number of layers and film thickness varied among the 3 sets from 4 layers to 10 layers, having nominal total thicknesses of 200, 120, and 50 nm, corresponding to individual layers of 50, 20, and 5 nm, respectively. Subsequently, the Au electrode was deposited on the uppermost organic layer, thus completing the assembly required for measurement of electrical properties. The electrical characterizations included capacitance–voltage (C–V) and current density–voltage (J–V) measurements for alternating thin layers of the –COOH and $-NH_2$ polymers sandwiched between the p-Si substrate and the top Au electrode, in a metal-insulator-semiconductor (MIS) capacitor configuration.

Figure 4A shows a typical C–V response of a 10-layer stack of alternating allyl amine (5 nm) and vinylacetic acid (5 nm) at 1 MHz frequency in a bias ranging from −5 V to 5 V. The high frequency response clearly shows accumulation at negative bias voltage and depletion regions at positive bias voltage. The k of this structure was extracted from the measured accumulation capacitance, based on the capacitance formula for a parallel capacitor,

$$\kappa = C \cdot t/\varepsilon_0 \quad (1)$$

where C is the accumulation capacitance per unit area (F cm^{-2}) and ε_0 is the permittivity of vacuum. The k extracted here was 6.21 at 1 MHz. The inset of Figure 4A shows the hysteresis behavior of the capacitor, exhibiting ca. 3.0 V hysteresis at 1 MHz due to uniformly distributed charges trapped in the polymer films during plasma deposition process.[15] As the total thickness of the capacitors is increased, a large hysteresis is observed. For each 4- and 6-layer stack of polymer film structure, a shift (Δ) of about 15 V and 7.2 V is observed, respectively. For all capacitors tested here, the trap charge density (N_t) in the dielectric layer is estimated to be ca. 10^{12} cm^{-2} using the relation

$$N_t = C \cdot \Delta/q \quad (2)$$

where q is the magnitude of electronic charge. The higher accumulation capacitance tends to shift to higher values when decreasing the frequency for all capacitors, as shown in Figure 4B. A frequency-dependent dispersion in the accumulation region is observed. The frequency dependence of k is

© 2008 WILEY-VCH Verlag GmbH & Co. KGaA, Weinheim

ADVANCED MATERIALS

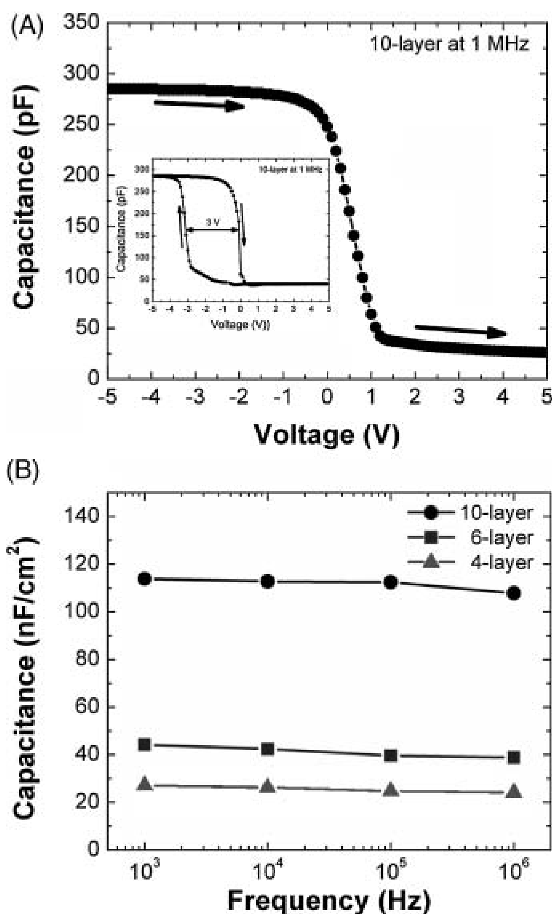

Figure 4. A) C–V characteristics of MIS capacitor at 1 MHz for a multilayer stack of plasma polymerized allyl amine (PP-AA) and vinylacetic acid (PP-VAA) film (Au/p-Si/10-layer stack of PP-AA and PP-VAA/Au). The inset shows the hysteresis behavior of the sample. B) Frequency dependence of the accumulation capacitance for the three different films in four orders of magnitude over frequency.

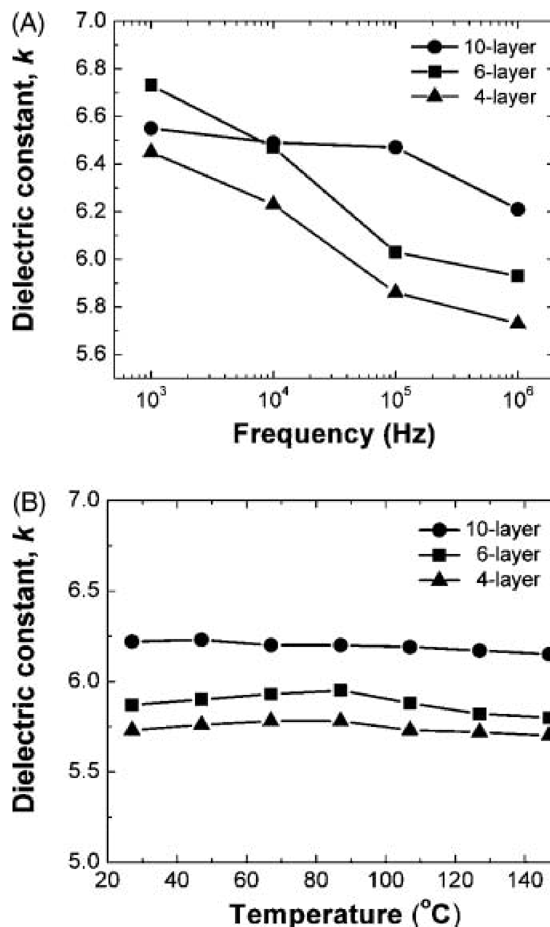

Figure 5. A) The dielectric constant k estimated from C–V measurement of a multilayer stack of plasma-polymerized allyl amine (PP-AA) and vinylacetic acid (PP-VAA) film as a function of frequency. B) The dielectric constant k of three multilayer stacked films studied here as a function of temperature at 1 MHz.

attributed to the slow polarization of the plasma-polymerized multilayer stack at higher frequencies and this polarization can lead to an increase in the induced charge at lower frequencies.[16] Under zero bias the dielectric loss at 1 MHz of the 4-, a 6-, and a 10-layer stack was (0.06 ± 0.001), (0.02 ± 0.001), and (0.02 ± 0.001), respectively.

The k of multilayer stacks was calculated for four different frequencies, as shown in Figure 5A. The phenomenon of higher k at lower frequency is observed. For a 10-layer stack, the dielectric constant varied from 6.21 at 1 MHz to 6.55 at 1 KHz. Similar behavior was observed for each 4- and 6-layer stack of polymer layers. The variation of k does not show any trend with varying the total thickness and number of multilayers, indicating that the thickness and the number of multilayers of the deposited films are not significant for controlling k. This phenomenon can be explained by the simulation results reported by Natori et al. when the ε is independent of thickness for $\varepsilon < 10$.[17] The dielectric constants of the three multilayer stacked films studied here show a small temperature dependence from 27 °C to 147 °C, indicating a good thermal stability of their dielectric constants, as shown in Figure 5B.

Figure 6 illustrates the J–V characteristics of multilayer stacks. As the total thickness of a multilayer film is decreased, the leakage current density is significantly reduced. The leakage current density of a metal–insulator–semiconductor (MIS) capacitor with 10-layer stack was 6.5 μA cm^{-2} at 1 MV cm^{-1}, which is two orders of magnitude smaller than the 6-layer stack film, and showed no breakdown over the voltage range shown in Figure 6. It should be noted that all the devices in this study were measured without any post-deposition annealing.[18] The inset of Figure 6 shows the hysteresis behavior of the J–V characteristics for a 10-layer stack of polymer films. Some hysteresis is observed in alternating forward and backward voltage sweeps. A leakage current density at 1 MV cm^{-2} is decreased two orders of magnitude when the total thickness of film is decreased, while increasing the number of multilayers in the stack, indicating that the number of interfaces within each deposited film is a more

© 2008 WILEY-VCH Verlag GmbH & Co. KGaA, Weinheim

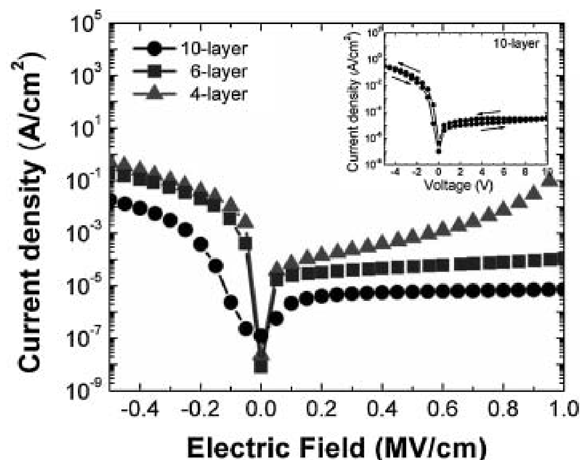

Figure 6. *J–V* characteristic for three different films without postdeposition annealing at room temperature. The inset shows the hysteresis behavior in the *J–V* curves for 10-layer stack film of plasma polymerized allyl amine (PP-AA) and vinylacetic acid (PP-VAA) film.

important factor to control the leakage current density in multilayer stacked bipolar polymer films than the aggregate thickness.

Under pulsed RF plasma polymerization conditions, efficient retention of monomer functional groups in the polymer film has been demonstrated.[18,19] In this experiment, it is confirmed that a significant number of $-COO^-$ and $-NH_3^+$ polar entities, generated from the interaction of the polyvinylacetic acid and the polyallyl amine films, is present in the layered polymer films as shown by XPS and ATR FT-IR analysis. The k values, in the range of 5.7–6.2 at 1 MHz obtained without any post-deposition annealing, are relatively high for purely organic films containing only oxygen and nitrogen as heteroatoms. These high k values are attributed to the unique multilayer stack of alternating layers, combined with the significant presence of $-COO^-$ and $-NH_3^+$ polar entities that induce strong dipole orientation polarizability. The redistribution of charges within a functional group with a net permanent dipole moment reorients itself in space in response to an external applied electric field. The relationship between ε and the total polarazibility (α) is often described by the Clausius–Mossotti relationship. The α is generally additive, including electronic, atomic, and dipole orientation polarizability and, within the context of the Clausius–Mossotti relationship, can be used to estimate the contribution of each polarization group to the dielectric constant.[20] The total polarizability increases when dipole orientation polarizability increases. As a result, k also increases. In this experiment, the observed small variation of k with varying the total thickness and number of multilayer stack suggests that the k is mainly due to the high dipole orientation polarizability induced between alternating charged layers.

In conclusion, a multilayer stack of polymeric thin films composed of alternating amine and carboxylic acid functional groups was deposited by pulsed RF plasma polymerization produced a composite structure having a relatively high k and low leakage current density as obtained without post-deposition annealing. This high-performance multilayer polymer film stack, deposited at ambient temperature and not subjected to further treatment of any kind, is promising in terms of use as a flexible dielectric material.

Experimental

Pulsed Plasma Deposition of Bipolar Film: A carboxylic acid (–COOH)-containing monomer, vinylacetic acid (VAA), and an amine ($-NH_2$)-containing monomer, allyl amine (AA), were polymerized under pulsed plasma operational conditions. For pulsed plasma deposition of VAA, a plasma duty cycle of 2/30 (plasma on-time, ms/plasma off-time, ms) was used at a monomer pressure 160 mTorr (1 Torr = 1.333×10^2 Pa) and 150 W power input. Allyl amine was plasma-polymerized at a duty cycle 10/30, monomer pressure 70 mTorr and 100 W power input. The polymer films were deposited on metal–insulator–semiconductor (MIS) substrates, which were assembled and cleaned, as described below. A bell-jar-shaped reactor, previously described, [13] was employed for the plasma depositions. A polymeric thin film of allyl amine was first plasma-deposited onto the substrate, which was then followed by the deposition of polyvinylacetic acid. The sequential deposition of AA and VAA films was performed to obtain a multistacked layered structure containing polar groups localized at the interfaces between each consecutive layer. Plasma deposition time was varied to control the thickness of the deposited films. Initial studies, using profilometry, revealed that deposition rates of both monomers varied linearly with deposition time under the pulsed plasma conditions employed. From the deposition rates measured, it was possible to control both the VAA and AA film thickness to desired values by use of appropriate deposition times.

Characterization of Bipolar Film: The number of layers and film thickness varied among the 3 sets from 4 layers to 10 layers, having nominal total thicknesses of 200, 120, and 50 nm, corresponding to individual layers of 50, 20, and 5 nm, respectively. For the 10, 6, and 4 layer thin films, the refractive index was estimated to be 1.55, 1.58, and 1.67, respectively, as measured by single wavelength ellipsometry. The flexibility property of the films was examined by SEM analysis of the films deposited on thin PMMA substrates. No cracking or delamination was noted after repeated flexing of the samples through 30° angles.

Fabrication of a Capacitor: MIS capacitors were fabricated on 2″ Boron-doped (100) p-type Si wafers with a resistivity of 4.2–4.4 Ω cm. The substrates were processed through standard degreasing and RCA cleaning procedures prior to plasma polymerization. After deposition of multilayer stacks of thin films was carried out under pulsed RF plasma conditions, the Au back contact (100 nm) were then electron beam evaporated in a low pressure range on the back side of the Si wafer. The MIS capacitors were completed by shadowmask electron beam evaporation (ca. 10^{-7} Torr) of the Au electrode, about 100 nm thick, directly onto the multilayer stack surface. The final MIS structure fabricated was a Au/p-Si/10-layer stack of PP-AA and PP-VAA/Au. The active area of each MIS capacitor studied was 0.283 mm^2.

Electrical Characterization: Capacitance–voltage (*C–V*) measurements were carried out with an LCR meter (Agilent 4284A) coupled with CSM/Win analysis software (Material Development Corporation, MA) at a frequency range from 1 KHz to 1 MHz at room temperature under darkness. For *C–V* measurements, the MIS capacitors were biased from $-t/10$ V to $+t/10$ V with voltage step of 0.1 V, where t is the total thickness (nm) of multilayer film. The hysteresis behaviors of the MIS capacitors were recorded at a frequency of 1 MHz. A correction procedure was employed to compute the series resistance of MIS capacitor. Current density–voltage (*J–V*) measurements were

 © 2008 WILEY-VCH Verlag GmbH & Co. KGaA, Weinheim

ADVANCED MATERIALS

performed with a semiconductor parameter analyzer (Agilent 4156) at room temperature. All capacitors fabricated were tested without any post-deposition annealing.

Received: November 29, 2007
Revised: January 23, 2008
Published online: May 26, 2008

[1] A. Facchetti, M. H. Yoon, T. J. Marks, *Adv. Mater.* **2005**, *17*, 1705.
[2] J. Veres, S. D. Ogier, S. W. Leeming, D. C. Cupertino, S. M. Khaffat, *Adv. Funct. Mater.* **2003**, *13*, 199.
[3] R. Parashkov, E. Becker, G. Ginev, T. Riedl, H. H. Johannes, W. Kowalsky, *J. Appl. Phys.* **2004**, *95*, 1594.
[4] J. Park, S. Y. Park, S. Shim, H. Kang, H. H. Lee, *Appl. Phys. Lett.* **2004**, *85*, 3283.
[5] H. G. O. Sandberg, T. G. Bäcklund, R. Österbacka, H. Stubb, *Adv. Mater.* **2004**, *16*, 1112.
[6] T. B. Singh, F. Meghdadi, S. Günes, N. Marjanovic, G. Horowitz, P. Lang, S. Bauer, N. S. Sariciftci, *Adv. Mater.* **2005**, *17*, 2315.
[7] M.-H. Yoon, A. Facchetti, T. J. Marks, *Proc. Natl. Acad. Sci. USA* **2005**, *102*, 4678.
[8] Y. Bai, Z. Y. Cheng, V. Bharti, H. S. Xu, Q. M. Zhang, *Appl. Phys. Lett.* **2000**, *76*, 3804.
[9] Z. M. Dang, Y. Shen, C. W. Nan, *Appl. Phys. Lett.* **2002**, *81*, 4814.
[10] Y. Shen, Y. Lin, M. Lin, C. W. Nan, *Adv. Mater.* **2007**, *19*, 1418.
[11] J. Hu, C. Yin, H.-Q. Mao, K. Tamada, W. Knoll, *Adv. Funct. Mater.* **2003**, *13*, 692.
[12] J. Zhang, X. Feng, H. Xie, Y. Shi, T. Pu, Y. Guo, *Thin Solid Films* **2003**, *435*, 108.
[13] D. Bhattacharyya, K. Pillai, O. M. R. Chyan, L. Tang, R. B. Timmons, *Chem. Mater.* **2007**, *19*, 2222.
[14] O. M. R. Chyan, J. J. Chen, F. Xu, J. Wu, *Anal. Chem.* **1997**, *69*, 2434.
[15] J. E. Klemberg-Sapieha, S. Sapieha, M. R. Wertheimer, A. Yelon, *Appl. Phys. Lett.* **1980**, *37*, 104.
[16] P. J. Brown, H. Sirringhaus, M. Harrison, M. Shkunov, R. H. Friend, *Phys. Rev. B* **2001**, *63*, 1252041.
[17] K. Natori, D. Otani, N. Sano, *Appl. Phys. Lett.* **1998**, *73*, 632.
[18] Y. Xu, P. R. Berger, J. Cho, R. B. Timmons, *J. Electron. Mater.* **2004**, *33*, 1240.
[19] J. Zhang, X. Feng, H. Xie, Y. Shi, T. Pu, Y. Guo, *Thin Solid Films* **2003**, *435*, 108.
[20] G. Hougham, G. Tesoro, A. Viehbeck, J. D. Chapple-Sokol, *Macromolecules* **1994**, *27*, 5964.

 © 2008 WILEY-VCH Verlag GmbH & Co. KGaA, Weinheim